Lyapunov Optimization in Online Battery Energy Storage System Control for Commercial Buildings

Jie Shi, *Member, IEEE*, Zuzhao Ye, *Student Member, IEEE*, H. Oliver Gao, and Nanpeng Yu, *Senior Member, IEEE*

***Abstract*—The high instantaneous discharging capability of battery energy storage systems (BESSs) make them ideal candidates for reducing peak loads in commercial buildings. An efficient online BESS control algorithm can be beneficial for reducing the monthly electricity bill of individual commercial buildings. Conventional model-based BESS control algorithms rely heavily on accurate long-horizon net load forecast, which is difficult to obtain. To address this problem, we develop a Lyapunov optimization-based online BESS control algorithm and derive its theoretical performance bound. Comprehensive numerical study results using real world commercial building smart meter data in southern California show that our proposed Lyapunov optimization-based online control algorithm with time-varying weighting parameters yields higher savings in electricity cost and requires less computation time in comparison to the state-of-the-art baseline algorithms.**

***Index Terms*—Battery energy storage system, stochastic optimization, Lyapunov optimization, commercial building.**

I. Introduction

BATTERY energy storage system (BESS) deployment has been growing rapidly in the United States over past years [1]. Commercial building managers have shown great interest in adopting BESSs due to their capabilities in shaving peak load and reducing electricity cost [2], [3]. As prices of battery packs continue to drop in the near future, the adoption rate of BESS in commercial buildings is expected to grow significantly. For better cost savings, online BESS control algorithms are needed to determine the battery charging and discharging signals based on the real-time building net load data. An efficient online BESS control algorithm can be crucial for reducing both the energy and demand charge components of the electricity bill of a commercial building.

BESSs are usually integrated with renewable energy resources, such as rooftop solar panels in commercial buildings [4]. This makes the design of a BESS control algorithm for an individual commercial building more challenging due to the high volatility and uncertainty in both electric load and renewable generation. Widely used control algorithms such as model predictive controls (MPCs) depend heavily on accurate net load forecasts. However, it is challenging to develop accurate net load forecasts that match typical billing cycles. To tackle this challenge, we seek to develop an efficient online BESS control algorithm for a commercial building that does not require any net load forecast. The control objective is to minimize the electricity bill which includes the energy charge and the demand charge.

Unlike residential buildings, the electricity bills of commercial buildings in the United States are highly dependent on the maximum power consumption and the peak demand charge within a monthly billing cycle. For commercial buildings with rooftop solar systems, the demand charges account for a significant portion of electricity bills. A commercial building's demand charge is usually proportional to its monthly peak load. The monthly peak load is highly volatile for an individual commercial building due to substantial variability in weather, building occupancy, and renewable generation. The presence of excessive uncertainties make it challenging to develop a BESS control algorithm that minimizes both energy and demand charge in a single commercial building in practice.

The topic of battery energy storage management for buildings has been extensively studied in the literature. Most of the previous research can be divided into two groups based on the BESS control objectives. The first group of work focuses on the BESS management for buildings that do not have demand charge. The goals of the BESS control algorithms are usually to minimize the costs (or equivalently maximize the benefits) for the target buildings, although the specific objectives can be diverse. For example, simple rule-based BESS control policies are introduced to shave the peak loads of residential buildings [5], [6], thereby reducing the energy costs. Stochastic optimization-based BESS control algorithms are developed to minimize energy costs [7], [8] and maximize economic gains [9] for residential buildings. Deterministic model predictive control algorithms based on forecasts are also proposed to minimize the operating costs of the target buildings [10], [11], [12]. An integrated management strategy for both renewable generation and BESS with controllable loads modeled by Markovian processes is developed in [13] to reduce the energy costs of residential buildings. [14] presents an adaptive control algorithm based on load forecasts to operate BESSs of residential building clusters so as to shave the peak load. To reduce energy costs of a residential building, the BESS control problem is solved using a reinforcement learning (RL) approach with cyclic time-dependent Markov process [15]. The problem of energy cost reduction in residential buildings with distributed energy resources is solved by multi-agent RL [16]. It is worth noting that the adoption of BESSs in buildings may not always be cost effective for all cases. For instance, [17] shows BESSs might not be economical due to the high investment cost and short lifetime.

J. Shi, Z. Ye and N. Yu are with the Department of Electrical and Computer Engineering, University of California, Riverside, CA 92501 USA. e-mail: nyu@ece.ucr.edu (Corresponding author: Nanpeng Yu)

H. O. Gao is with the Department of Systems Engineering, Cornell University, Ithaca, NY 14853 USA. e-mail: hg55@cornell.edu

The second group of work develops BESS control algorithms for buildings with both energy charge and demand charge incurred. Since the demand charge often accounts for a significant portion of the electricity bill, methods with a focus on peak load shaving [18], [19], [20] have been developed to reduce the electricity bill for commercial buildings. However, peak load shaving alone is not necessarily sufficient for electricity bill minimization in buildings with large energy consumption. To address this problem, [21] proposed an optimization algorithm that reduces the peak load and the daily energy cost separately. Many researchers proposed joint optimization algorithms to reduce the electricity costs for commercial buildings. For example, peak load shaving [22] and energy cost reduction [23] are jointly optimized given benefits from providing ancillary services to the power grid. An optimal coordination algorithm to provide energy arbitrage, frequency regulation, and spinning reserve services for buildings with energy storage resources is developed [24].

More relevant to our work, [25], [26], [3], [27] developed MPC-based BESS management approaches that jointly minimize energy charge and demand charge for individual commercial buildings. MPC-based approaches require accurate forecast of future electric loads and renewable generation, which can be very difficult to obtain for a single commercial building due to the high uncertainty and long prediction horizon. The demand charge, which depends on the peak load within the monthly billing cycle, is extremely sensitive to prediction model, hence prone to forecast errors. This problem becomes more pronounced for small size commercial buildings with irregular operation schedules. To address the net load uncertainties, Lyapunov optimization-based control algorithms have been developed for BESS management in various applications, such as optimal demand response [28], operational cost reduction of a data center [29], optimal utility scheduling of a power-harvesting network [30], long term operational cost minimization of a microgrid [31], customer energy cost reduction [32], [33], [34], and efficient routing of an energy hub [35]. Nevertheless, none of existing studies investigate the long-horizon joint minimization of energy charge and demand charge for a commercial building. Similar previous studies, for example [33] and [34], only consider residential buildings without demand charge. The energy charge is simply a sum of immediate electricity consumption costs billed at each time step. The demand charge, which is proportional to the peak power, can only be determined at the end of the billing cycle. The introduction of demand charge brings additional complexity in both problem formulation and solution method that needs to be investigated and addressed rigorously, being the primary motivation of this study. To bridge this research gap, we propose a Lyapunov optimization-based online BESS control algorithm to reduce the monthly electricity bill of a commercial building. Our approach does not require any prior information of future electric load or renewable generation associated with the target commercial building. Instead, it attempts to strike a balance between immediate cost and resource reservation at each time step. For example, the proposed approach is likely to release more battery energy to reduce the immediate cost when it goes relatively high and charge the battery when the immediate cost appears to be low.

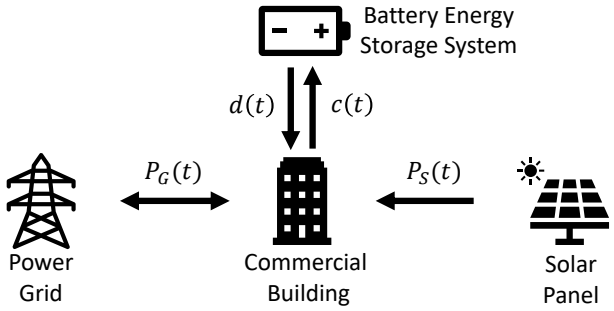

Fig. 1: Diagram of a commercial building with solar PV generation and BESS.

The contributions of this work are summarized as below:

- We formulate the online BESS control problem for a single commercial building as a stochastic optimization problem with the goal to minimize both monthly demand charge and energy charge.
- We develop not only a Lyapunov optimization-based online control algorithm to solve the stochastic optimization problem but also the corresponding performance bounds.
- Comprehensive numerical study results using real world commercial building smart data show that the proposed Lyapunov optimization-based control algorithm with multiple weighting parameters achieves not only lower electricity cost but also shorter computation time than state-of-the-art baseline algorithms.

The rest of this paper is organized as the following: Section II presents the formulation of the BESS control problem for a single commercial building. Section III discusses the technical details of the proposed Lyapunov optimization-based control algorithm and its performance bounds. Section IV evaluates the proposed framework with several numerical studies based on net load data from a real world commercial building in southern California. Section V concludes this study.

II. Problem Formulation

In this section, we formulate the management of BESS for a commercial building as a stochastic programming problem. The objective of the optimization problem is to minimize the monthly electricity bill of the commercial building through efficient control of the BESS.

Fig. 1 shows the high level schematic diagram of the commercial building's energy system being studied. The commercial building has access to three power sources: the solar panel, the BESS, and the power grid. The direction of energy flows follows the rules below:

- The electric energy flow between the commercial building and the power grid is bidirectional.
- The electric energy flow between the commercial building and the BESS is bidirectional.
- The electric energy can only flow from the solar panel to the commercial building.

Note that if the electric energy generated by the solar panel is greater than the building energy demand, then the extra electric energy has to go to either the power grid or the BESS.

In the next two subsections, we present the components of the monthly electricity bill and the system operation constraints in the proposed control framework. The stochastic programming problem is formulated in the last subsection.

A. Monthly Electricity Bill of Commercial Buildings

The monthly electricity bill of a commercial building in the United States usually includes two parts: the energy charge and the demand charge. The energy charge of the building in different time-of-use periods are proportional to the quantity of electricity consumed in the corresponding periods. The demand charge is proportional to the maximum power drawn by the building from the grid within a billing cycle. Let $C_E(m)$ and $C_D(m)$ denote the energy charge and the demand charge of a given commercial building in month m. Then $C_E(m)$ and $C_D(m)$ can be formulated as:

$$C_E(m) = \Delta T \sum_{t=1}^{T} [p_E(t) \max(P_G(t), 0) + p_F(t) \min(P_G(t), 0)] \tag{1}$$

$$C_D(m) = p_D \quad \max(f0, P_G(t) j t = 1, \quad , Tg), \tag{2}$$

where T is the total number of control time intervals in a given month. ΔT is the length of each time interval. $p_E(t)$ is the price of electricity sold to the commercial building at time step t. $P_G(t)$ denotes the power transferred between the grid and the commercial building. The sign of $P_G(t)$ defines the direction of electric energy flow. Positive $P_G(t)$ indicates the electric energy flows from the grid to the commercial building. $p_F(t)$ is the price of electricity sold back to the grid by the commercial building at time step t. p_D denotes the demand charge rate.

The sum of $C_E(m)$ and $C_D(m)$ is the electricity bill of a commercial building for a given month m, which is denoted by $EB(m)$:

$$EB(m) = C_E(m) + C_D(m). \tag{3}$$

Note that the calculation of $C_E(m)$ follows net metering policy, which allows the building to offset retail electricity purchase using output from on-site distributed energy resources. Thus, $C_E(m)$ could be negative when the benefit from the solar generation outweighs the energy cost. $p_F(t)$ can be set as zero if no credit is provided by feeding electricity back to the grid. If the load factor of the building is small, then the demand charge $C_D(m)$ can dominate the electricity bill. Finally, if the battery degradation costs can be clearly quantified, it can also be included in the objective function. In this study, we assume the battery degradation cost to be marginal, hence not included.

B. Operational Constraints

In this subsection, we formulate the operational constraints of the BESS control and optimization problem.

1) Power grid: The distribution lines connecting buildings and the power grid have limited capacities, which limit the power transfer between the commercial building and the power grid as follows:

$$P_{bound} \quad P_G(t) \quad P_{bound}, \tag{4}$$

where P_{bound} is a positive constant. Note that we could easily modify the constrain if the maximum energy inflow and outflow limits are different.

2) Battery Energy Storage System: A battery energy storage system has its maximum capacity which can degrade over time. To slow down the degradation process, the actual usable range of the BESS is usually set below the maximum capacity [3], yielding the following constraint:

$$E_{min} \quad E(t) \quad E_{max} \tag{5}$$

where $E(t)$ is the remaining energy of BESS at time step t. E_{min} and E_{max} are the minimum and maximum values of the remaining energy of BESS, respectively.

The BESS also has maximum charging/discharging rate, which is determined by both the battery materials and the power electronic components. The two constraints below model the charging and discharging rate limits of the BESS:

$$0 \quad c(t) \quad P_{max} \tag{6}$$

$$0 \quad d(t) \quad P_{max}, \tag{7}$$

where $c(t)$ and $d(t)$ are the charging and discharging power at time step t. Note that the formulation can be extended to consider different maximum charging and discharging power.

Based on the above definitions, the dynamics of the remaining energy of BESS can be represented by the following state transition equation derived from [36]:

$$E(t+1) = E(t) + [c(t) \quad d(t)] \quad \Delta T \quad \underbrace{j d(t) \quad c(t) j \, \Delta T \quad (1 \quad p_{\overline{\kappa}})}_{\text{Energy loss}}, \tag{8}$$

where κ denotes the round-trip efficiency of the entire BESS. The round-trip efficiency is defined as the percentage of electricity put into storage that is later retrieved. The higher the round-trip efficiency, the less energy is lost in the storage process [37]. The last term on the right hand side of the above equation accounts for the energy loss during each time interval.

When the remaining energy of the BESS approaches the boundaries of the usable range, additional constraints on the charging/discharging rate need to be enforced:

$$\Delta T \quad c(t) \quad p_{\overline{\kappa}} \quad E_{max} \quad E(t) \tag{9}$$

$$\Delta T \quad d(t) \quad (2 \quad p_{\overline{\kappa}}) \quad E(t) \quad E_{min} \tag{10}$$

It is worth noting that these two inequalities are equivalent to energy storage constraint $E_{min} \quad E(t+1) \quad E_{max}$. Please refer to Appendix A for details.

3) Electric Power Balance: According to the law of conservation of energy, the following relationship among the load and different energy sources can be derived as (Fig. 1):

$$P_G(t) = L_B(t) \quad P_S(t) + c(t) \quad d(t), \tag{11}$$

where $L_B(t)$ denotes the electric load of the commercial building at time step t. $P_S(t)$ is measures the electric power generated by the solar panel at time step t. Note that $L_B(t)$ is always greater than or equal to zero.

C. Stochastic Programming Problem

In the real-world, the electric load of a commercial building is affected by various random factors such as the weather condition and the number of occupants. The solar generation is also subject to significant uncertainties caused by the time-varying cloud cover and ambient temperature. Therefore, the electric load of the commercial building $L_B(t)$ and solar generation $P_S(t)$ are treated as random variables with unknown distributions in this study.

The energy charge $C_E(m)$ and the demand charge $C_D(m)$ of the building for month m are also random variables due to the uncertain electric load and solar generation. To account for the uncertainties, the objective of BESS control problem is to minimize the expectation of the monthly electricity bill $EB(m)$. The stochastic programming problem for BESS control is formulated as:

$$\begin{aligned} \underset{c(t),d(t)}{\text{minimize}} \quad & \mathsf{E}[C_E(m) + C_D(m)] \\ \text{subject to} \quad & (4) \quad (11) \end{aligned} \tag{12}$$

It is difficult to obtain the global optimal BESS control policy because of the deep uncertainties introduced by the long control/optimization horizon of a month and the unknown distributions of $L_B(t)$ and $P_S(t)$. In next section, we will present an online BESS control strategy using Lyapunov optimization, which can find a satisfactory sub-optimal solution to the stochastic programming problem.

III. Technical Methods

In this section, we propose a Lyapunov optimization-based approach to control BESS in real-time operations by solving the stochastic programming problem formulated in previous section. In Lyapunov optimization, a Lyapunov function is leveraged to control a dynamical system. The proposed approach does not require any information about the distribution of electric load and solar generation and can be implemented easily as an online algorithm. We refer the interested readers to [38] for a detailed discussion of Lyapunov optimization. In the following subsections, we present the technical details of the proposed BESS control strategy based on Lyapunov optimization.

A. Battery Energy Queue

Lyapunov optimization was first introduced to optimize the management of queueing systems. It aims to strike a balance between system performance and queue congestion. Regarding the proposed BESS control problem, the depth of discharge (DoD) of the BESS can be considered as a queue backlog. The goal of Lyapunov optimization-based control strategy is to maintain a good balance between BESS's DoD and immediate energy costs.

To fit our problem into the Lyapunov optimization framework, a queue needs to be defined. In this study, we define a queue $Q(t)$ as:

$$Q(t) = E_{max} \quad E(t) \quad \Delta T \quad P_{max} \quad \overline{p}_{\kappa}. \tag{13}$$

We call $Q(t)$ the battery energy queue, which indicates the amount of discharged energy. To comply with the BESS usable range defined by (5), $Q(t)$ should be restricted as follows:

$$P_{max}\Delta T\overline{p}_{\kappa} \quad Q(t) \quad E_{max} \quad E_{min} \quad P_{max}\Delta T\overline{p}_{\kappa} \tag{14}$$

The purpose of introducing the term $\Delta T \; P_{max} \; \overline{p}_{\kappa}$ is to ensure that the BESS's energy level never exceeds E_{max}, which will be explained in detail in Section III-C.

Based on the dynamics of remaining BESS energy (8) and the definition of queue (13), the update of $Q(t)$ can be calculated by:

$$\begin{aligned} Q(t+1) = Q(t) + [d(t) \quad c(t)] \quad \Delta T \\ + j d(t) \quad c(t) j \; \Delta T \quad (1 \quad \overline{p}_{\kappa}) \end{aligned} \tag{15}$$

Note that the last two terms on the right hand side (RHS) of the above equation only depend on the control variables. Let $U(t)$ denote the input as the sum of the two RHS terms. The above equation can be simplified as:

$$Q(t+1) = Q(t) + U(t) \tag{16}$$

The proposed queue can also be interpreted as an indicator of battery size requirement. Suppose we do not impose any limit on E_{max} and let $Q(t)$ evolve with the input $U(t)$, then the maximum value of $Q(t)$ will determine the required capacity of the BESS. A larger maximum value of $Q(t)$ corresponds to a larger capacity of the BESS.

B. Lyapunov Optimization-Based BESS Control

The goal of Lyapunov optimization is to achieve a low overall operation cost in the long run by making reasonable trade-off between immediate cost and queue backlog for each time interval. In this work, the queue backlog is equivalent to the battery energy queue $Q(t)$. The immediate commercial building energy cost $g(t)$ at each time step t includes both immediate energy charge and corresponding control action's contribution to the total demand charge. In this study, $g(t)$ is computed as:

$$\begin{aligned} g(t) = \underbrace{\Delta T \quad [p_E(t) \quad \max(P_G(t), 0) + p_F(t) \quad \min(P_G(t), 0)]}_{\text{Immediate energy charge}} \\ + \underbrace{p_D \quad \max(0, P_G(t) \quad M(t))}_{\text{Immediate demand charge}}, \end{aligned} \tag{17}$$

where $M(t) = \max\left(M(t \quad 1), P_G(t \quad 1)\right), \forall t = 1, 2, \quad , T$ and $M(0) = M_{ini}$. With the notations defined above, we can see that the sum of the initial demand charge and the cumulative immediate building energy cost is equal to the electricity bill of the commercial building:

$$p_D \quad M_{ini} + \sum_{t=1}^{T} g(t) = C_E(m) + C_D(m) \tag{18}$$

The immediate cost $g(t)$ can be divided into two parts:

The first part is the immediate energy charge, which is simply the energy cost for one time interval. It is determined by the electricity prices and electric energy consumption. The sum of all the immediate energy charges across all time steps in a given month m equals $C_E(m)$.

The second part is the immediate demand charge. It measures the increase in demand charge due to the increased peak demand. Similarly, the sum of $p_D \quad M_{ini}$ and all the immediate demand charges in a given month m gives $C_D(m)$.

Note that M_{ini} is a tunable hyperparameter. The average daily peak demand in previous month could be a good initial value.

Following the typical Lyapunov optimization framework [38], we define a quadratic Lyapunov function $L(t)$ as:

$$L(t) = \frac{1}{2}Q(t)^2 \tag{19}$$

The primary reason for using quadratic Lyapunov function is that, when computing the change in the Lyapunov function from one slot to the next, the quadratic Lyapunov function has important dominant cross terms that include an inner product of queue backlogs and transmission rates [38]. Note this Lyapunov function is non-negative by definition. Then, the one-slot conditional Lyapunov drift can be derived as:

$$\Delta L(t) = \mathsf{E}[L(t+1) \quad L(t)|Q(t)]. \tag{20}$$

The Lyapunov drift describes the expected change of the Lyapunov function over one time interval. In the proposed BESS control problem, this term indicates the change of BESS's DoD. The following Lemma provides an upper bound of the Lyapunov drift.The proof of Lemma 1 is presented in Appendix B.

Lemma 1. *The one-slot conditional Lyapunov drift $\Delta L(t)$ satisfies the following inequality $\forall t$:*

$$\Delta L(t) \quad B + Q(t)\mathsf{E}[U(t)|Q(t)], \tag{21}$$

where $B = \frac{1}{2}[\Delta T \quad P_{max} + 2\Delta T \quad P_{max} \quad (1 \quad p_{\overline{\kappa}})]^2$

Recall that the core idea of Lyapunov optimization is to strike a balance between immediate cost and queue backlog variation. To this end, the following optimization problem based on Lyapunov drift $\Delta L(t)$ and immediate cost $g(t)$ is formulated at each time step to determine the control signals.

$$\begin{aligned} \underset{c(t),d(t)}{\text{minimize}} \quad & \Delta L(t) + V \quad \mathsf{E}(g(t)|Q(t)) \\ \text{subject to} \quad & (6) \text{ and } (7) \end{aligned} \tag{22}$$

The objective function (22) is called *drift-plus-penalty*, which is a weighted sum of the Lyapunov drift and the expected immediate cost given current queue backlog. V is a weighting parameter. However, we can not directly solve the above optimization problem due to the presence of Lyapunov drift. To convert the optimization problem into a tractable one, we show that there exists an upper bound of the *drift-plus-penalty*. We then minimize this upper bound instead of the *drift-plus-penalty*. In the next subsection, we present the converted problem and show that it can be efficiently solved online.

C. Online BESS Control Algorithm

First, let $\Delta J(t)$ denote the objective function in (22). By following **Lemma 1**, the inequality below always holds:

$$\Delta J(t) \quad B + Q(t)\mathsf{E}[U(t)|Q(t)] + V \quad \mathsf{E}(g(t)|Q(t)) \tag{23}$$

For an arbitrary time step t_a, the above equation can be reduced to a deterministic expression by observing $L_B(t_a)$, $P_S(t_a)$, and $E(t_a)$:

$$\Delta J(t_a) \quad B + Q(t_a) \quad U(t_a) + V \quad g(t_a) \tag{24}$$

Now, our goal is to obtain the BESS's control signals by minimizing this upper bound:

$$\begin{aligned} \underset{c(t_a),d(t_a)}{\text{minimize}} \quad & Q(t_a) \quad U(t_a) + V \quad g(t_a) \\ \text{subject to} \quad & (6) \text{ and } (7), \end{aligned} \tag{25}$$

where $U(t_a)$, $g(t_a)$, and $P_G(t_a)$ can be derived as:

$$\begin{aligned} U(t_a) = {} & [d(t_a) \quad c(t_a)] \quad \Delta T \\ & + |d(t_a) \quad c(t_a)| \, \Delta T \quad (1 \quad p_{\overline{\kappa}}) \end{aligned} \tag{26a}$$

$$\begin{aligned} g(t_a) = {} & \Delta T \quad p_E(t_a) \quad \max(P_G(t_a), 0) \\ & + \Delta T \quad p_F(t_a) \quad \min(P_G(t_a), 0) \\ & + p_D \quad \max(0, P_G(t_a) \quad M(t_a)) \end{aligned} \tag{26b}$$

$$P_G(t_a) = L_B(t_a) \quad P_S(t_a) + c(t_a) \quad d(t_a) \tag{26c}$$

Note that (25) can be considered as a continuous piece-wise linear function with respect to a single variable $[d(t_a) \quad c(t_a)]$. Therefore the global optimum of this converted optimization problem can be efficiently found by comparing the values of change points and endpoints.

Note that the queue backlog $Q(t)$ corresponds to the discharged battery energy, which is physically constrained by the BESS capacity. Now we need to select the weighting parameter V for trade-off between queue backlog reduction and immediate cost. The following theorem claims that $Q(t)$ satisfies the physical constraint for all time intervals if V is set within proper range. The proof of Theorem 1 is presented in Appendix C.

Theorem 1. *If the immediate cost $g(t)$ is finite at each time step, then the following inequality with respect to queue backlog $Q(t)$ and weighting parameter V holds for all time steps:*

$$Q(t) \quad \frac{V \quad (g_{max} \quad g_{min})}{\Delta T \quad P_{max}} p_{\overline{\kappa}}, \tag{27}$$

where g_{min} and g_{max} are the lower bound and upper bound of $g(t)$, respectively.

It is worth noting that the tightness of this bound on $Q(t)$ depends on the distribution of $g(t)$. An extreme case would be $g(t) = g_{max} = g_{min}, \forall t$. In this scenario, $g(t)$ is independent of control variables. The queue backlog $Q(t)$ will remain 0 at the corresponding bound.

Meanwhile, we can also derive a lower bound of $Q(t)$, which is denoted by Q_L. Note that $U(t)$ is monotonically increasing with respect to $[d(t) \quad c(t)]$. $g(t)$ is monotonically decreasing with respect to $[d(t) \quad c(t)]$. Therefore, once $Q(t) < 0$, $U(t)$ will be positive by solving (25), leading to

increase of $Q(t)$ at next time step. Given that our system is a discrete system, it is possible that $Q(t)$ goes from a positive value to a negative value between two subsequent time steps. Clearly, such negative value is bounded by the minimum value of $U(t)$. Therefore, the following inequality holds:

$$Q(t) \quad Q_L = \quad \Delta T \quad P_{max} \quad \underline{p}_{\overline{\kappa}} \tag{28}$$

As $\Delta T \;!\; 0$, $Q_L \;!\; 0$. This lower bound gives rise to the introduction of $\Delta T \quad P_{max} \quad \underline{p}_{\overline{\kappa}}$ into (13), which ensures the BESS's energy level $E(t)$ never exceeds E_{max}.

The proposed online BESS control algorithm does not require any prior information or forecasts of future uncertainties. It seeks to maintain a balance between system performance and resource reserved for unknown look-ahead perturbations regardless of time interval length. Regarding the proposed BESS control problem, the remaining energy of the BESS can be considered as available resource. The goal of Lyapunov optimization-based control strategy is to maintain a good balance between BESS's remaining energy and immediate energy costs. In other words, it sacrifices certain immediate benefits based on current states in return for delayed rewards, which explains its fundamental logic in handling future uncertainties.

D. Theoretical Performance of Online BESS Control Policy

It is desirable to analyze the theoretical performance of the proposed BESS control strategy with respect to the optimal control policy. In this subsection, we derive an upper bound for the difference between the expected electric bill of the commercial building under the proposed control approach and the theoretical optimum.

By taking expectation on both sides of (18), we have:

$$p_D \quad M_{ini} + \sum_{t=1}^{T} \mathsf{E}[g(t)] = \mathsf{E}[C_E(m) + C_D(m)] \tag{29}$$

The RHS of the above equation is exactly the objective function of the original stochastic optimization problem. Given that $p_D \quad M_{ini}$ is a constant, the value of $\sum_{t=1}^{T} \mathsf{E}[g(t)]$ thereby determines the performance of a BESS control policy. The following theorem provides an upper bound for the difference between the performance of the proposed BESS control strategy and the global optimum. The proof of Theorem 2 is presented in Appendix D.

Theorem 2. *Let π be an optimal control policy that minimizes (12). Let π^g be the proposed control policy. Let $Q\ (t)$ and $L\ (t)$ be the queue backlog and Lyapunov function under the optimal control policy π , respectively. Suppose $L_B(t)$ and $P_S(t)$ are i.i.d. over different time steps. Then the following inequality holds:*

$$\sum_{t=1}^{T} \mathsf{E}[g_{\pi^g}(t)] \quad \sum_{t=1}^{T} \mathsf{E}[g_{\pi}\ (t)] + \frac{T \quad C}{V} + \frac{L\ (1)}{V}, \tag{30}$$

where $g_{\pi^g}(t)$ is the immediate cost under the proposed control policy π^g. $g_{\pi}\ (t)$ is the immediate cost under the optimal control policy π . $C = B + {P_{max}}^2 \Delta T^2 \kappa$.

Note that if C is very large, then this upper bound on the performance difference might not be very tight. Nevertheless, selecting a large value of V can help improve the performance of the proposed online BESS control algorithm. Recall that the queue backlog $Q(t)$ and V are inversely proportional to each other in (42). An excessively large V can lead to a $Q(t)$ that is beyond the feasible range. Thus, there exists a trade-off between BESS control algorithm performance and the required capacity for $Q(t)$. Selecting a good value of V is, therefore, the key to the successful application of the proposed control approach.

To conclude, the proposed Lyapunov optimization-based control strategy has several pros and cons. First, the proposed approach does not require any load forecasting or prior information of future electric load profile. Second, it is extremely lightweight and computationally efficient, which can be easily deployed on embedded controllers. Third, the proposed Lyapunov optimization-based control strategy only has one hyperparameter, making the tuning process relatively easy. The major con of the proposed Lyapunov optimization-based control strategy is its sensitivity regarding the hyparparameter V. The numerical studies in the next section will demonstrate that the performance of the proposed approach is highly dependent on the value of V.

IV. Numerical Study

In this section, we evaluate the proposed Lyapunov optimization-based online BESS control algorithm using real-world data collected from a commercial building in southern California. We start from analyzing the impact of hyperparameter V on control performance so as to identify the proper value for V. Then, we compare the monthly electricity bills achieved by the proposed control approach and the selected baseline algorithms. Finally, we analyze the impact of control time interval and the scalability of the proposed control algorithm.

A. Numerical Setup

1) Data Source: In this study, we use the net load data of the Children Center of San Diego State University, which is located in San Diego, California. This commercial building is equipped with solar panels. The net load data are sampled every 15 minutes from April 2021 to July 2021. Fig. 2 shows the net load profile of April 2021. Note that the negative net loads indicate backfeed of electricity into the power distribution network.

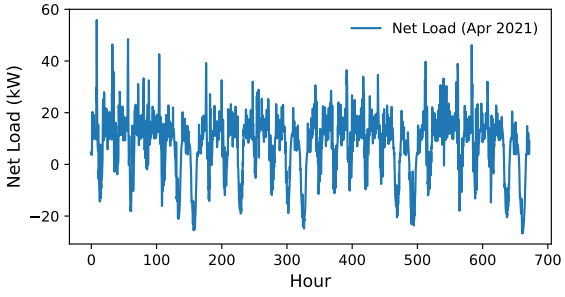

Fig. 2: Net load of the commercial building in April 2021.

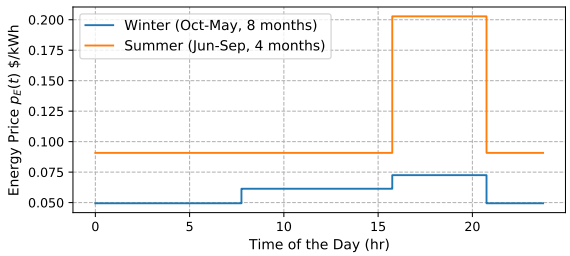

Fig. 3: Electricity prices during winter and summer months.

TABLE I: System Parameters

Parameter	Value	Unit
Bound of grid power P_{bound}	60	kW
Maximum charging speed P_{max}	60	kW
Maximum battery energy E_{max}	270	kWh
Minimum battery energy E_{min}	30	kWh
Round-trip efficiency κ	0.88	-
Initial state of charge SoC_{ini}	0.5	-
Initial value of $M(t)$ M_{ini}	20	kW
Control time interval T	15 , 30, 60	min

* T = 15 minutes is the default control time interval except otherwise noted.

2) System Parameters: The prices of energy charge $p_E(t)$ and demand charge $p_D(t)$ are obtained from an electric utility in southern California [39]. Specifically, $p_E(t)$ varies with time-of-use periods and seasons, as shown in Fig. 3. Under the net-metering program, the price of electricity sold back to the grid is the same as the purchasing price, i.e. $p_F(t) = p_E(t)$. The demand charge price p_D is \$9.39/kW monthly. Other system parameters such as charging/discharging limits, battery energy capacity, efficiency, and control time interval are listed in Table I.

3) Baseline Methods: We select the theoretical optimal control solution and two MPC schemes as baseline algorithms for comparison purpose. The optimal control solution can be obtained by solving the optimization problem (12) with constraints (4)-(11) and the exact information of future loads. The first MPC baseline algorithm solves the same optimization problem with 7-day rolling windows and predicted future net loads. We adopt a simple yet effective prediction approach called similar-day method, which directly uses electric load data of the previous week as the forecast for the next week. Given electric load data has strong weekly seasonality, load profiles between two adjacent weeks can be quite similar to each other. This simple prediction method is surprisingly powerful in many cases [40]. We also include an ideal MPC method as a baseline where the net load forecasts are replaced with ground-truth values.

B. Selection of V for Lyapunov Optimization

The selection of proper V values is crucial for the success of the proposed BESS control approach as discussed in Section III-D. Here, we analyze the impact of V values on the monthly electricity bills obtained by the proposed method. We will start from using a single V value throughout the control process and then discuss how the performance can be improved by using two different V values for peak and non-peak periods.

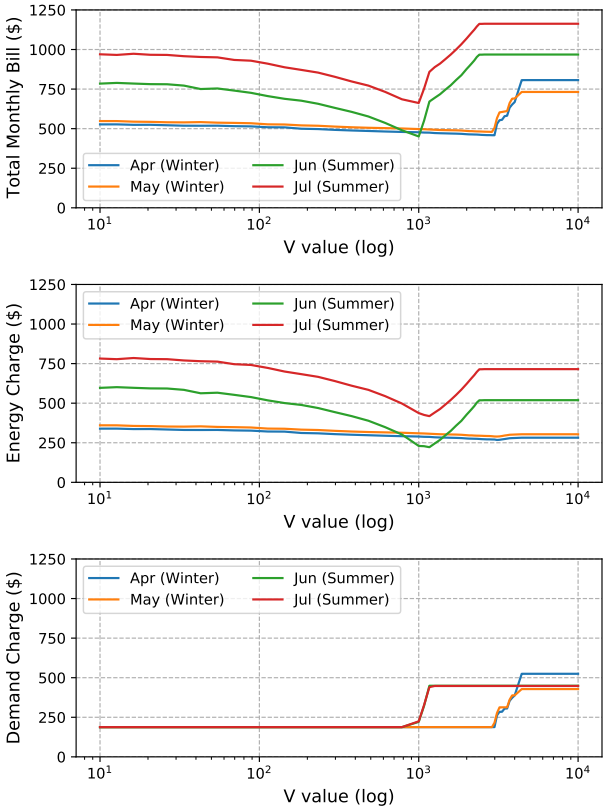

Fig. 4: Total monthly electricity bills (top), energy charge C_E (middle), and demand charge C_D (bottom) obtained by the proposed approach under different single V values.

1) Single V: In this case, we use the same V value throughout the control process. We gradually increase the value of V starting from 10. As shown in Fig. 4, the total monthly electricity bill decreases as V increases and then bounces up when V becomes too large. Through further visualizing the energy charge C_E and demand charge C_D, we find that the impacts of V can be split into two regimes. Taking the summer months (Jun and Jul) for example, when V increases but is below 10^3, the energy charge C_E is gradually reduced and the demand charge C_D is kept the same. On the other hand, when V is above 10^3, both C_E and C_D are found to increase with V. This result matches our theoretical analysis in Section III-D that increased value of V within certain range can help improve the performance when the corresponding queue backlog is within the feasible operating range. When V becomes too large, the required queue backlog size will exceed the limit of the BESS capacity. The performance bound provided by Theorem 2 is no longer valid in this scenario. The performance of the proposed control strategy dramatically degrades due to the lack of balance between remaining battery

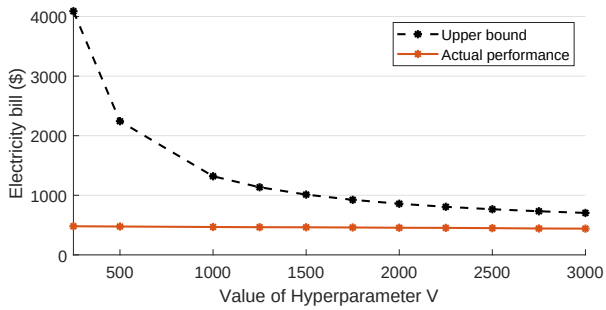

Fig. 5: Actual performance and theoretical upper bound with various values of V in April, 2021.

energy and the instantaneous energy cost.

We record the actual performance and the derived upper bound of the proposed approach with various values of hyperparameter V using the electric load data of the target commercial building in April, 2021. Fig, 5 shows the actual performance and the theoretical upper bound given different values of V. Clearly, the theoretical bound appears to be tighter as the value of V increases.

Note that in summer months the monthly electricity bills are most sensitive to the change in V, as indicated by the slopes of curves in Fig. 4 when $V < 10^3$. This implies that it is more difficult to select a proper value of V for the summer months. In practical applications, we can address this issue by using multiple values of V for different hours in a day as discussed below.

2) Multiple Vs: We notice that the electricity price differences between peak and non-peak hours during summer months are much larger than that of winter months. Recall that V is a weighting factor that balances the remaining battery energy and the instantaneous energy cost. Therefore, we should use higher values of V during peak hours to reduce the immediate energy cost and lower V values during non-peak hours to incentivize the replenishment of battery energy.

Fig. 6 shows the 2-D heatmaps of the monthly bills by using two different values of V for peak and non-peak hours. First, it is observed that months within the same season show similar performance patterns across different values of V. The white dashed lines correspond to the results using a single fixed value of V. Clearly, the performance of the proposed approach is more sensitive to V in summer months compared to that in winter months. This is consistent with our observation of the single V case. Most importantly, we identify the regions of V value combinations that consistently achieve low electricity bills. For winter months, we can select V for peak hours roughly in the 2 10^3 3 10^3 range, and V for non-peak hours in the 1 10^1 1 10^3 range. Similarly, for summer months, we can select V in the 8 10^2 1 10^3 range for peak hours and the 1 10^1 1 10^2 range for non-peak hours to achieve consistently good control performance.

Without loss of generality, we will use fixed values of V in the following performance comparison. The fixed values of V are listed in Table II.

TABLE II: Selected Values of V

V	**Winter**	**Summer**
Peak Hours	2.5 10^3	1 10^3
Non-peak Hours	5 10^2	5 10^1

C. Electricity Bill Comparison

The performance of the Lyapunov optimization-based control policy is compared with other baseline methods in Fig. 7. We observe significant electricity bill reduction by adopting the proposed Lyapunov-based BESS control policy throughout the four months in comparison to the original electricity bills without BESS.

The electricity cost reduction is more pronounced in summer months than that in winter months. It is worth noting that the monthly electricity bills obtained by the Lyapunov optimization-based control policy are lower than that of the MPC method for all four months. Moreover, the Lyapunov optimization-based control policy can achieve a performance close to the theoretical optimum during the winter months. Specifically, the electricity bill under the proposed approach is only 112% and 110% of the theoretical minimum in April and May, respectively. For the summer months, these ratios become larger (226% and 159% for June and July, respectively) due to the increased electricity price variation during the day. The ideal MPC approach can efficiently handle this price variation assuming that perfect net load forecasts for the entire month are available. Nevertheless, the ideal MPC results are unattainable in practice because of the existence of load forecasting errors. Table III displays the average root mean square error (RMSE) of the load forecasting for each month in this study. It is worth noting that obtaining an accurate electric load forecast of a single commercial building is usually difficult due to the high randomness of events and weather conditions, making the MPC-based approaches less effective. By comparison, the proposed approach does not have this issue by virtue of its zero dependency on prior information of future load profile.

Recall that we assumed net-metering rates in the previous analysis. However, consider the sustainable development of the grid, the sell-back price $p_F(t)$ shall be less than the purchasing price $p_E(t)$ to compensate for the additional costs of the grid (e.g. infrastructure and management). To demonstrate if the proposed method is still effective in asymmetrical rates, we further consider the following three scenarios:

Net-metering, i.e. $p_F(t) = p_E(t)$,
The selling price is 5% less than the purchasing price, i.e. $p_F(t) = 0.95p_E(t)$,
The selling price is 30% less than the purchasing price, i.e. $p_F(t) = 0.70p_E(t)$.

In Fig. 8, the electricity bill (Apr 2021) is shown under different control methods and pricing schemes. From the figure we can see that with the widening of the gap between selling and purchasing prices, the total electricity bills are raised in all five methods. However, the rises are all limited, even in

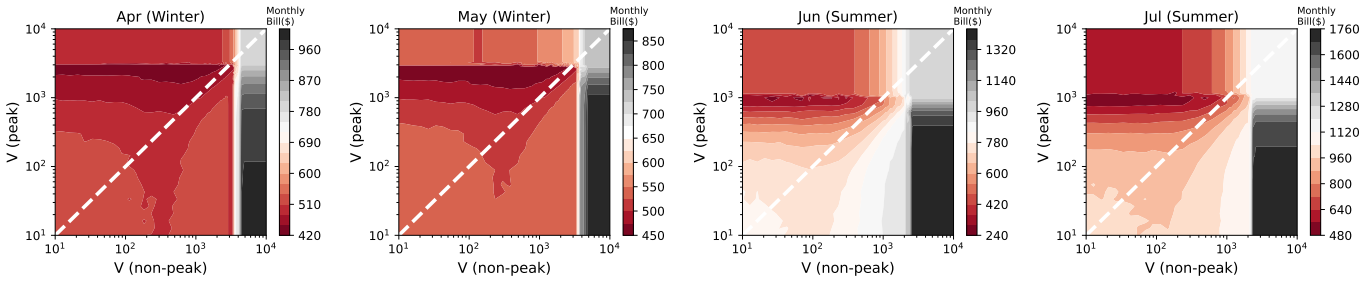

Fig. 6: Monthly electricity bills obtained by the proposed approach using two different values of V for peak hours and non-peak hours.

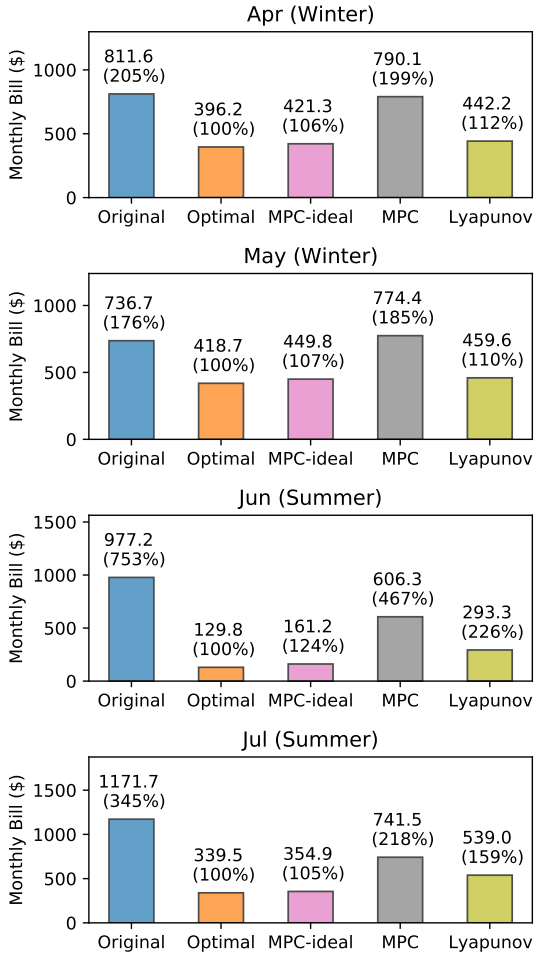

Fig. 7: Comparison of monthly electricity bills under different control policies.

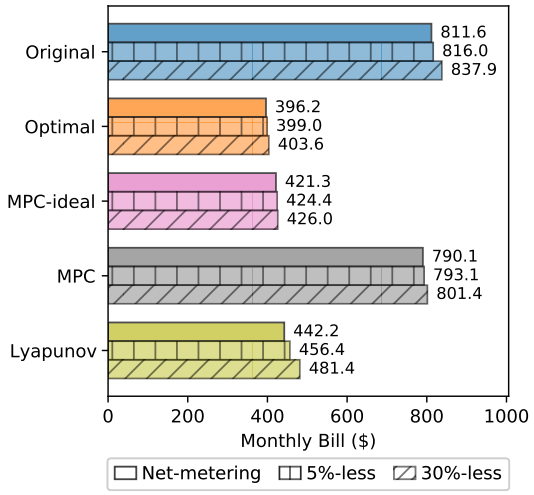

Fig. 8: Comparison of the electricity bill (Apr 2021) under different control policies and pricing schemes.

TABLE III: Average RMSE of load forecasting error for each month.

Month	April	May	June	July
Average RMSE (kW)	8.39	8.83	9.84	9.39

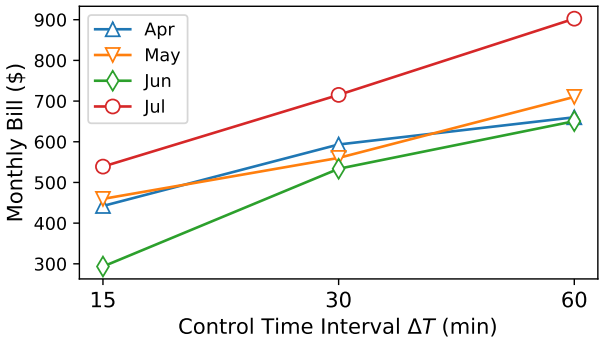

Fig. 9: Comparison of monthly electricity bills with different control time intervals.

the extreme case where the selling price is 30% less than the purchasing price. This phenomenon indicates that the proposed method, as well as other baseline methods, is capable of handling the asymmetrical rates. This is in line with our expectation as the proposed method explicitly differentiated selling and purchasing prices in (26b).

D. Impact of Control Time Interval

In the above analysis, we select $\Delta T = 15$ minutes as the default control time interval, which is the same as the

TABLE IV: Comparison of Computational Time per Step with Different Control Time Intervals

Control Time Interval	Computation Time per Step (s)	
	MPC	Lyapunov
T = 60min	4.0	
T = 30min	8.9	1.0 10 5
T = 15min	20.1	

data sampling interval. It is interesting to investigate how the performance of the proposed BESS control algorithm changes when a different time interval is selected. Note that when calculating the electricity bills for a different control time interval, the demand charge still needs to be calculated based on the 15-minute interval data as it is determined by the electric utility company. We re-evaluate the control experiments with $\Delta T = 30$ and 60 minutes. The results are shown in Fig. 9. The monthly electricity bills increase when we use a larger control time interval for all four months.

Note that the data sampling frequency can be increased in practical applications, where the Lyapunov optimization-based control policy is expected to achieve even lower monthly electricity bills. More importantly, the adoption of a shorter control time interval barely affects the computation time of the proposed algorithm. We record the computation time per step for the MPC-based method and Lyapunov optimization-based control policy under different control time intervals in Table IV. The computation time of the MPC-based method is roughly a million times larger than that of the Lyapunov optimization-based control policy. Moreover, the computation time doubles when the control time interval is reduced by half for the MPC-based method. Meanwhile, for the proposed approach, the computation time almost remains the same when the control time interval is shortened. This test result shows the great advantage of using Lyapunov optimization-based control policy with more granular control time intervals.

V. Conclusion

This paper develops an efficient online control algorithm for battery energy storage system based on Lyapunov optimization to reduce the electricity bill of an individual commercial building. The proposed control strategy helps reduce both the energy charge and the demand charge of the commercial building in a billing cycle (month). The proposed control algorithm seeks to find an appropriate trade-off between the remaining battery energy and the instantaneous energy cost in each control interval. Neither prior information nor forecasts of future net loads are required for the proposed control algorithm. Numerical results with real world building data show that the proposed Lyapunov optimization-based control algorithm not only yields higher energy cost savings but also consumes computation time magnitudes less than that of the baseline algorithm.

Acknowledgment

This research project is supported by the California Energy Commission under Agreement Number EPC-19-053.

Appendix A
Proof of the Equivalence of Energy Storage Constraint and Inequalities (9) and (10).

In this appendix, we prove that the energy storage constraint E_{min} $E(t+1)$ E_{max} is equivalent to inequalities (9) and (10). Eq. (8) describes the transition of remaining energy in the battery:

$$E(t+1) = E(t) + [c(t) \quad d(t)] \quad \Delta T \quad jd(t) \quad c(t)j \ \Delta T \quad (1 \quad p_{\overline{\kappa}}) \tag{31}$$

Therefore, E_{min} $E(t+1)$ E_{max} indicates:

$$E_{min} \quad E(t) + [c(t) \quad d(t)] \quad \Delta T \quad jd(t) \quad c(t)j \ \Delta T \quad (1 \quad p_{\overline{\kappa}}) \quad E_{max} \tag{32}$$

If the battery is being discharged, then $d(t)$ 0 and $c(t) = 0$:

$$E_{min} \quad E(t) \quad d(t) \quad \Delta T(2 \quad p_{\overline{\kappa}}) \quad E_{max} \tag{33}$$

Note $E(t)$ $d(t)$ $\Delta T(2$ $p_{\overline{\kappa}})$ E_{max} is always satisfied because $d(t)$ 0. The above inequality is thereby equivalent to:

$$d(t) \quad \Delta T(2 \quad p_{\overline{\kappa}}) \quad E(t) \quad E_{min} \tag{34}$$

If the battery is being charged, then $d(t) = 0$ and $c(t)$ 0:

$$E_{min} \quad E(t) + c(t) \quad \Delta T p_{\overline{\kappa}} \quad E_{max} \tag{35}$$

Note E_{min} $E(t) + c(t)$ $\Delta T p_{\overline{\kappa}}$ is always satisfied because $c(t)$ 0. The above inequality is thereby equivalent to:

$$c(t) \quad \Delta T p_{\overline{\kappa}} \quad E_{max} \quad E(t) \tag{36}$$

Therefore, the energy storage constraint E_{min} $E(t+1)$ E_{max} is equivalent to inequalities (9) and (10).

Appendix B
Proof of Lemma 1

Lemma 1. *The one-slot conditional Lyapunov drift $\Delta L(t)$ satisfies the following inequality for all t:*

$$\Delta L(t) \quad B + Q(t)\mathbb{E}[U(t)jQ(t)], \tag{37}$$

where $B = \frac{1}{2}[\Delta T \quad P_{max} + 2\Delta T \quad P_{max} \quad (1 \quad p_{\overline{\kappa}})]^2$.

Proof. Based on (19), we have:

$$\begin{aligned} L(t+1) \quad L(t) &= \frac{1}{2}\left[Q(t+1)^2 \quad Q(t)^2\right] \\ &= \frac{1}{2}\Big\{\left[E_{max} \quad E(t+1) \quad \Delta T \quad P_{max} \quad \overline{p}_{\kappa}\right]^2 \\ &\qquad \left[E_{max} \quad E(t) \quad \Delta T \quad P_{max} \quad \overline{p}_{\kappa}\right]^2\Big\} \\ &= \frac{1}{2}\left\{E(t+1)^2 \quad E(t)^2 + 2(E_{max} \quad \Delta T \right. \\ &\qquad \left. P_{max} \quad \overline{p}_{\kappa})\left[E(t) \quad E(t+1)\right]\right\} \\ &= \frac{1}{2}[E(t+1) \quad E(t)][E(t+1) + E(t) \\ &\qquad 2(E_{max} \quad \Delta T \quad P_{max} \quad \overline{p}_{\kappa})] \\ &= \frac{1}{2}[E(t+1) \quad E(t)]\left[2E(t) \quad U(t) \right. \\ &\qquad \left. 2\left(E_{max} \quad \Delta T \quad P_{max} \quad \overline{p}_{\kappa}\right)\right] \\ &= U(t)[Q(t) + \frac{1}{2}U(t)] \\ &= \frac{1}{2}U(t)^2 + U(t)Q(t) \end{aligned} \tag{38}$$

Given (6) and (7), an upper bound of $U(t)$ can be derived:

$$U(t) \quad \Delta T \quad P_{max} + \Delta T \quad P_{max} \quad (1 \quad \overline{p}_{\kappa}) \tag{39}$$

By substituting (39) into (38), we have:

$$\begin{aligned} L(t+1) \quad L(t) \quad \frac{1}{2}\left[\Delta T \quad P_{max} + \Delta T \quad P_{max} \right. \\ \left. (1 \quad \overline{p}_{\kappa})\right]^2 + U(t)Q(t) \end{aligned} \tag{40}$$

Taking conditional expectation on both sides yields:

$$\begin{aligned} \Delta L(t) \quad & \underbrace{\frac{1}{2}\left[\Delta T \quad P_{max} + \Delta T \quad P_{max} \quad (1 \quad \overline{p}_{\kappa})\right]^2}_{B} \\ & + Q(t)\mathsf{E}[U(t)|Q(t)] \end{aligned} \tag{41}$$

□

APPENDIX C
PROOF OF THEOREM 1

Theorem 1. *If the immediate cost $g(t)$ is finite at each time step, then the following inequality with respect to queue backlog $Q(t)$ and weighting parameter V holds for all time steps:*

$$Q(t) \quad \frac{V \quad (g_{max} \quad g_{min})}{\Delta T \quad P_{max} \quad \overline{p}_{\kappa}}, \tag{42}$$

where g_{min} and g_{max} are the lower bound and upper bound of $g(t)$, respectively.

Proof. Let $a(t) = [d(t_a) \quad c(t_a)] + d(t_a) \quad c(t_a)$ (1 $\overline{p}_{\kappa}$). Based on (6) and (7), we have:

$$P_{max} \quad \overline{p}_{\kappa} \quad a(t) \quad P_{max} \quad (2 \quad \overline{p}_{\kappa}) \tag{43}$$

In the proposed online BESS control algorithm, the following objective function is minimized at each time step t:

$$obj(a(t)) = \Delta T \quad Q(t) \quad a(t) + V \quad g(t) \tag{44}$$

Let's assume $Q(t) = \epsilon + R$, where $\epsilon > 0$ and R satisfies:

$$\Delta T \quad R \quad P_{max} \quad \overline{p}_{\kappa} + V \quad g_{max} = V \quad g_{min} \tag{45}$$

Note that $g_{min} \quad g(t) \quad g_{max}, \forall t$. Then, the following two arguments hold:

For any $a(t) = a^+ \quad 0$, we have $obj(a^+) \quad V \quad g_{min}$. Let $a \quad$ be the optimal solution. For $a(t) = \quad P_{max} \quad \overline{p}_{\kappa}$, we have:

$$\begin{aligned} obj(a \;) \quad & obj(\quad P_{max} \quad \overline{p}_{\kappa}) \\ &= \quad \Delta T \quad Q(t) \quad P_{max} \quad \overline{p}_{\kappa} + V \quad g(t) \\ &= \quad \Delta T \quad (\epsilon + R) \quad P_{max} \quad \overline{p}_{\kappa} + V \quad g(t) \\ &= \quad \Delta T \quad \epsilon \quad P_{max} \quad \overline{p}_{\kappa} \quad \Delta T \\ &\quad R \quad P_{max} \quad \overline{p}_{\kappa} + V \quad g(t) \\ &< V \quad g_{min} \end{aligned} \tag{46}$$

These two arguments indicate the optimal solution $a \quad$ has to be negative in this situation. In other words, once the queue backlog $Q(t) \quad \epsilon + R$, it will decrease at the following time step. Let $\epsilon \; ! \; 0$, we have $Q(t) \quad R$. Substituting (45) into R yields:

$$Q(t) \quad \frac{V \quad (g_{max} \quad g_{min})}{\Delta T \quad P_{max} \quad \overline{p}_{\kappa}} \tag{47}$$

□

APPENDIX D
PROOF OF THEOREM 2

Theorem 2. *Let $\pi \quad$ be an optimal control policy that minimizes (12). Let π^g be the proposed control policy. Let $Q\ (t)$ and $L\ (t)$ be the queue backlog and Lyapunov function under the optimal control policy π , respectively. Suppose $L_B(t)$ and $P_S(t)$ are i.i.d. over different time steps. Then the following inequality holds:*

$$\sum_{t=1}^{T} \mathsf{E}[g_{\pi^g}(t)] \quad \sum_{t=1}^{T} \mathsf{E}[g_{\pi} \;(t)] + \frac{T \quad C}{V} + \frac{L \;(1)}{V}, \tag{48}$$

where $g_{\pi^g}(t)$ is the immediate cost under the proposed control policy π^g. $g_{\pi}\ (t)$ is the immediate cost under the optimal control policy π . $C = B + P_{max}{}^2\Delta T^2\kappa$.

Proof. Based on **Lemma 1**, we have:

$$\begin{aligned} \Delta L\ (t) + V\mathsf{E}[g_{\pi^g}(t)|Q\ (t)] \quad & B + Q\ (t)\mathsf{E}[U_{\pi^g}(t)|Q\ (t)] \\ & + V\mathsf{E}[g_{\pi^g}(t)|Q\ (t)] \end{aligned} \tag{49}$$

Note that π^g minimizes $Q(t)\mathsf{E}[U(t)|Q(t)] + V\mathsf{E}(g(t)|Q(t))$ at each time step. Therefore, we have:

$$\begin{aligned} & Q\ (t)\mathsf{E}[U_{\pi^g}(t)|Q\ (t)] + V\mathsf{E}[g_{\pi^g}(t)|Q\ (t)] \\ & \quad Q\ (t)\mathsf{E}[U_{\pi}\ (t)|Q\ (t)] + V\mathsf{E}[g_{\pi}\ (t)|Q\ (t)] \end{aligned} \tag{50}$$

Combining (49) and (50) yields:

$$\begin{aligned} & \Delta L\ (t) + V\mathsf{E}[g_{\pi^g}(t)|Q\ (t)] \quad B \\ & \quad + Q\ (t)\mathsf{E}[U_{\pi}\ (t)|Q\ (t)] + V\mathsf{E}[g_{\pi}\ (t)|Q\ (t)], \end{aligned} \tag{51}$$

where $U_\pi\ (t)$ denotes the control input under π . Note that π is a feasible solution to the original stochastic programming problem (12). Therefore, $Q\ (t)$ satisfies the following bound:

$$P_{max}\Delta T\overline{p}_{\kappa} \quad Q\ (t) \quad E_{max} \quad E_{min} \quad P_{max}\Delta T\overline{p}_{\kappa} \tag{52}$$

We can also derive a bound for $\mathsf{E}[U_\pi\ (t)jQ\ (t)]$ based on (26a):

$$P_{max}\Delta T\overline{p}_{\kappa} \quad \mathsf{E}[U_\pi\ (t)jQ\ (t)] \quad P_{max}\Delta T(2 \quad \overline{p}_{\kappa}) \tag{53}$$

Given our only random variables $L_B(t)$ and $P_S(t)$ are i.i.d. over different time steps, there exists an optimal control policy that satisfies $\mathsf{E}[U_\pi\ (t)jQ\ (t)] \quad 0$ according to Theorem 4.5 in [38]. Combining this inequality with (52) and (53) yields:

$$Q\ (t)\mathsf{E}[U_\pi\ (t)jQ\ (t)] \quad P_{max}{}^2\Delta T^2\kappa \tag{54}$$

Let $C = B + P_{max}{}^2\Delta T^2\kappa$. Substituting (54) into (51) yields:

$$\Delta L\ (t) + V\mathsf{E}[g_{\pi^g}(t)jQ\ (t)] \quad C + V\mathsf{E}[g_\pi\ (t)jQ\ (t)] \tag{55}$$

Taking expectation over $Q\ (t)$ on both sides of (55) gives:

$$\mathsf{E}[L\ (t+1) \quad L\ (t)] + V\mathsf{E}[g_{\pi^g}(t)] \quad C + V\mathsf{E}[g_\pi\ (t)] \tag{56}$$

By summing (56) over $t = 1, 2, 3, \quad , T$, we have:

$$\mathsf{E}[L\ (T+1) \quad L\ (1)] + V\sum_{t=1}^{T}\mathsf{E}[g_{\pi^g}(t)] \quad T \quad C + V\sum_{t=1}^{T}\mathsf{E}[g_\pi\ (t)] \tag{57}$$

Rearranging the terms in the above equation yields:

$$\sum_{t=1}^{T}\mathsf{E}[g_{\pi^g}(t)] \quad \sum_{t=1}^{T}\mathsf{E}[g_\pi\ (t)] + \frac{T \quad C}{V} + \frac{\mathsf{E}[L\ (1)] \quad \mathsf{E}[L\ (T+1)]}{V} \tag{58}$$

Note that $L\ (1)$ is deterministic and $L\ (T+1) \quad 0$. Thus, we have:

$$\sum_{t=1}^{T}\mathsf{E}[g_{\pi^g}(t)] \quad \sum_{t=1}^{T}\mathsf{E}[g_\pi\ (t)] + \frac{T \quad C}{V} + \frac{L\ (1)}{V} \tag{59}$$

□

REFERENCES

[1] "Battery storage in the United States: An update on market trends," US Energy Information Administration (EIA), Tech. Rep., 2021. [Online]. Available: https://www.eia.gov/analysis/studies/electricity/batterystorage/pdf/battery_storage_2021.pdf

[2] J. A. McLaren, P. J. Gagnon, and S. Mullendore, "Identifying potential markets for behind-the-meter battery energy storage: A survey of US demand charges," National Renewable Energy Laboratory (NREL), Tech. Rep., 2017.

[3] Z. Zhang, J. Shi, Y. Gao, and N. Yu, "Degradation-aware valuation and sizing of behind-the-meter battery energy storage systems for commercial customers," in *2019 IEEE PES GTD Grand International Conference and Exposition Asia (GTD Asia)*. IEEE, 2019, pp. 895–900.

[4] K. Misbrener, "California Energy Commission mandates solar + storage on new commercial buildings," Aug. 2021. [Online]. Available: https://www.solarpowerworldonline.com/2021/08/california-energy-commission-mandates-solar-storage-new-commercial-buildings/

[5] J. Leadbetter and L. Swan, "Battery storage system for residential electricity peak demand shaving," *Energy and Buildings*, vol. 55, pp. 685–692, Dec. 2012.

[6] M. B. Roberts, A. Bruce, and I. MacGill, "Impact of shared battery energy storage systems on photovoltaic self-consumption and electricity bills in apartment buildings," *Appl. Energy*, vol. 245, pp. 78–95, Jul. 2019.

[7] F. Hafiz, A. R. de Queiroz, and I. Husain, "Multi-stage stochastic optimization for a PV-storage hybrid unit in a household," in *2017 IEEE Ind. Appl. Soc. Annu. Meet. IAS 2017*, Oct. 2017, pp. 1–7.

[8] F. Hafiz, M. Awal, A. R. de Queiroz, and I. Husain, "Real-time stochastic optimization of energy storage management using deep learning-based forecasts for residential PV applications," *IEEE Trans. Ind. Appl.*, vol. 56, no. 3, pp. 2216–2226, Jan. 2020.

[9] F. Conte, S. Massucco, M. Saviozzi, and F. Silvestro, "A stochastic optimization method for planning and real-time control of integrated PV-storage systems: design and experimental validation," *IEEE Trans. Sustain. Energy*, vol. 9, no. 3, pp. 1188–1197, Nov. 2017.

[10] Q. Yan, B. Zhang, and M. Kezunovic, "Optimized operational cost reduction for an EV charging station integrated with battery energy storage and PV generation," *IEEE Trans. Smart Grid*, vol. 10, no. 2, pp. 2096–2106, Jan. 2018.

[11] M. Tavakoli, F. Shokridehaki, M. F. Akorede, M. Marzband, I. Vechiu, and E. Pouresmaeil, "CVaR-based energy management scheme for optimal resilience and operational cost in commercial building microgrids," *Int. J. Electr. Power Energy Syst.*, vol. 100, pp. 1–9, Sep. 2018.

[12] J. Niu, Z. Tian, Y. Lu, and H. Zhao, "Flexible dispatch of a building energy system using building thermal storage and battery energy storage," *Appl. Energy*, vol. 243, pp. 274–287, Jun. 2019.

[13] M. Nistor and C. H. Antunes, "Integrated management of energy resources in residential buildings—A Markovian approach," *IEEE Trans. Smart Grid*, vol. 9, no. 1, pp. 240–251, Apr. 2016.

[14] Y. Wang, X. Lin, and M. Pedram, "Adaptive control for energy storage systems in households with photovoltaic modules," *IEEE Trans. Smart Grid*, vol. 5, no. 2, pp. 992–1001, Mar. 2014.

[15] S. Abedi, S. W. Yoon, and S. Kwon, "Battery energy storage control using a reinforcement learning approach with cyclic time-dependent markov process," *Int. J. Elect. Power & Energy Syst.*, vol. 134, p. 107368, 2022.

[16] M. Ahrarinouri, M. Rastegar, and A. R. Seifi, "Multiagent reinforcement learning for energy management in residential buildings," *IEEE Trans. on Ind. Informat.*, vol. 17, no. 1, pp. 659–666, 2020.

[17] Z. Xu, X. Guan, Q.-S. Jia, J. Wu, D. Wang, and S. Chen, "Performance analysis and comparison on energy storage devices for smart building energy management," *IEEE Trans. Smart Grid*, vol. 3, no. 4, pp. 2136–2147, Dec. 2012.

[18] A. Bar-Noy, M. P. Johnson, and O. Liu, "Peak shaving through resource buffering," in *International Workshop on Approximation and Online Algorithms*, Sep. 2008, pp. 147–159.

[19] A. Bar-Noy, Y. Feng, M. P. Johnson, and O. Liu, "When to reap and when to sow–Lowering peak usage with realistic batteries," in *International Workshop on Experimental and Efficient Algorithms*, May 2008, pp. 194–207.

[20] Y. Mo, Q. Lin, M. Chen, and S.-Z. J. Qin, "Optimal online algorithms for peak-demand reduction maximization with energy storage," in *Proc. ACM e-Energy*, 2021, pp. 73–83.

[21] B. Hartmann, D. Divényi, and I. Vokony, "Evaluation of business possibilities of energy storage at commercial and industrial consumers–A case study," *Appl. Energy*, vol. 222, pp. 59–66, Jul. 2018.

[22] Y. Shi, B. Xu, D. Wang, and B. Zhang, "Using battery storage for peak shaving and frequency regulation: Joint optimization for superlinear gains," *IEEE Trans. Power Syst.*, vol. 33, no. 3, pp. 2882–2894, Sep. 2017.

[23] S. Beer, T. Gómez, D. Dallinger, I. Momber, C. Marnay, M. Stadler, and J. Lai, "An economic analysis of used electric vehicle batteries integrated into commercial building microgrids," *IEEE Trans. Smart Grid*, vol. 3, no. 1, pp. 517–525, Feb. 2012.

[24] H. Hao, D. Wu, J. Lian, and T. Yang, "Optimal coordination of building loads and energy storage for power grid and end user services," *IEEE Trans. Smart Grid*, vol. 9, no. 5, pp. 4335–4345, Jan. 2017.

[25] A. J. Hasan, L. F. Enriquez-Contreras, J. Yusuf, and S. Ula, "A comprehensive building load optimization method from utility rate structure perspective with renewables and energy storage," in *SEST 2021 - 4th Int. Conf. Smart Energy Syst. Technol.* IEEE, 2021, pp. 1–6.

[26] M. J. Risbeck and J. B. Rawlings, "Economic model predictive control for time-varying cost and peak demand charge optimization," *IEEE Trans. Automat. Contr.*, vol. 65, no. 7, pp. 2957–2968, Sep. 2019.

[27] H. S. Zhou, R. Passey, A. Bruce, and A. B. Sproul, "Aggregated impact of coordinated commercial-scale battery energy storage systems on network peak demand, and financial outcomes," *Renew. Sust. Energ. Rev.*, vol. 144, p. 111014, Jul. 2021.

[28] L. Huang, J. Walrand, and K. Ramchandran, "Optimal demand response with energy storage management," in *IEEE Int. Conf. Smart Grid Commun. (SmartGridComm)*, Nov. 2012, pp. 61–66.

[29] R. Urgaonkar, B. Urgaonkar, M. J. Neely, and A. Sivasubramaniam, "Optimal power cost management using stored energy in data centers," in *Proceedings of the ACM SIGMETRICS Joint International Conference on Measurement and Modeling of Computer Systems*, Jun. 2011, pp. 221–232.

[30] L. Huang and M. J. Neely, "Utility optimal scheduling in energy-harvesting networks," *IEEE ACM Trans. Netw.*, vol. 21, no. 4, pp. 1117–1130, Dec. 2012.

[31] W. Shi, N. Li, C.-C. Chu, and R. Gadh, "Real-time energy management in microgrids," *IEEE Trans. Smart Grid*, vol. 8, no. 1, pp. 228–238, Aug. 2015.

[32] T. Li and M. Dong, "Real-time energy storage management with renewable energy of arbitrary generation dynamics," in *IEEE Asilomar Conf. Signals Syst. Comput.*, Nov. 2013, pp. 1714–1718.

[33] ——, "Real-time energy storage management with renewable integration: Finite-time horizon approach," *IEEE J. Sel. Areas Commun.*, vol. 33, no. 12, pp. 2524–2539, Sep. 2015.

[34] ——, "Real-time residential-side joint energy storage management and load scheduling with renewable integration," *IEEE Trans. Smart Grid*, vol. 9, no. 1, pp. 283–298, Apr. 2016.

[35] P. Li, W. Sheng, Q. Duan, Z. Li, C. Zhu, and X. Zhang, "A Lyapunov optimization-based energy management strategy for energy hub with energy router," *IEEE Trans. Smart Grid*, vol. 11, no. 6, pp. 4860–4870, Sep. 2020.

[36] B. Foggo and N. Yu, "Improved battery storage valuation through degradation reduction," *IEEE Transactions on Smart Grid*, vol. 9, no. 6, pp. 5721–5732, May 2017.

[37] A. Mey, "Utility-scale batteries and pumped storage return about 80% of the electricity they store," U.S. Energy Information Administration, Tech. Rep., Feb. 2021. [Online]. Available: https://www.eia.gov/todayinenergy/detail.php?id=46756#

[38] M. J. Neely, "Stochastic network optimization with application to communication and queueing systems," *Synthesis Lectures on Commun. Netw.*, vol. 3, no. 1, pp. 1–211, 2010.

[39] "Southern California Edison Schedule TOU-GS-2," accessed June 2021. [Online]. Available: https://library.sce.com/content/dam/sce-doclib/public/regulatory/tariff/electric/schedules/general-service-&-industrial-rates/ELECTRIC_SCHEDULES_TOU-GS-2.pdf

[40] R. Weron, *Modeling and forecasting electricity loads and prices: A statistical approach*. John Wiley & Sons, 2007.

Jie Shi (M'21) received the B.S. degree in Automation from Shenyang University of Technology, Shenyang, China in 2012. He received the M.S. degree in Control Theory & Control Engineering from Southeast University, Nanjing, China in 2015. He received the Ph.D. degree in Electrical and Computer Engineering from the University of California, Riverside, CA, USA in 2021. His research interests include smart infrastructure systems, intelligent systems, and machine learning.

Zuzhao Ye (S'20) received the B.E. degree in thermal energy and power engineering from the University of Science and Technology of China, Hefei, China, in 2015. He is currently pursuing the Ph.D. degree in electrical and computer engineering with the University of California at Riverside, Riverside, CA, USA. His research interests include big data analytics, machine learning, and optimization, particularly in their applications to the planning and operation of electric-vehicle charging infrastructure.

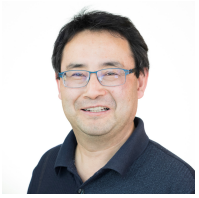

H. Oliver Gao Director of the Center for Transportation, Environment, and Community Health (CTECH), is the Howard Simpson Professor with the School of Civil and Environmental Engineering at Cornell University. Gao's research focuses on modeling and development of systems solutions for sustainable and intelligent infrastructure systems, low carbon and low emission transportation systems, and human-centered design for environment and public health. Gao received his graduate degrees (Ph.D. in Civil and Environmental Engineering, M.S. in Statistics, and M.S. in Agriculture and Resource Economics) from the University of California at Davis in 2004, M.S. degree in Civil Engineering in 1999, and duel undergraduate degrees in Environmental Science and Civil Engineering in 1996 from Tsinghua University, China.

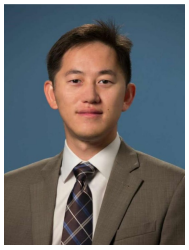

Nanpeng Yu (M'11-SM'16) received his B.S. in Electrical Engineering from Tsinghua University, Beijing, China, in 2006. Dr. Yu also received his M.S. and Ph.D. degree in Electrical Engineering from Iowa State University, Ames, IA, USA in 2007 and 2010 respectively. He is currently an Associate Professor in the department of Electrical and Computer Engineering and the Director of Energy, Economics, and Environment Research Center at University of California, Riverside, CA, USA. His current research interests include machine learning in smart grid, electricity market design and optimization, and smart energy communities. Dr. Yu is an Associate Editor of IEEE Transactions on Smart Grid and IEEE Transactions on Sustainable Energy.